Chinese Journal of Chemical Engineering 56 (2023) 160–168

Contents lists available at ScienceDirect

Chinese Journal of Chemical Engineering

journal homepage: www.elsevier.com/locate/CJChE

Full Length Article

Mechanistic insights into the active intermediates of 2,6-diaminopyridine dinitration

Junao Zhu [#], Zhirong Yang [#,*], Yuanhan Chen, Mingming Chen, Zhen Liu, Yueqiang Cao, Jing Zhang, Gang Qian, Xinggui Zhou, Xuezhi Duan [*]

State Key Laboratory of Chemical Engineering, School of Chemical Engineering, East China University of Science and Technology, Shanghai 200237, China

ARTICLE INFO

Article history:
Received 24 March 2022
Received in revised form 15 June 2022
Accepted 29 June 2022
Available online 9 July 2022

Keywords:
2,6-Diaminopyridine
Nitration mechanism
Active intermediates
Thermal effects
Negative water effects

ABSTRACT

Mechanistic understanding of the active intermediates of 2,6-diaminopyridine (DAP) dinitration in the concentrated nitric-sulfuric acid system is of crucial importance for the selectivity control of target product, *i.e.*, 2,6-diamino-3,5-dinitropyridine (DADNP). The active intermediates determining the product selectivity are theoretically studied. The HSO_4^--NO_2^+ complex is proposed as the dominant active nitrating intermediate for the first time, which shows low energy barrier (*i.e.*, 10.19 kcal·mol^{-1},1 kcal = 4.186 kJ) for direct dinitration of DAP to DADNP. The formed water during the reaction results in not only the formation of less active SO_4^{2-}-NO_2^+ complex, but also the occurance of DAP sulfonation (DAP-SO_3H intermediate) to facilitate the formation of mononitration byproduct. Meanwhile, the accompanied thermal effects cause the generation of undesirable pyridine-$NHNO_2$ intermediate, which is difficult to be rearranged to yield DADNP, inhibiting the reaction and thus giving low DAP conversion. The insights reported here elucidates the importance of thermal effects elimination and water content control, confirmed experimentally in the batch- and micro-reaction systems.

1. Introduction

Poly 2,5-dihydroxy-1,4-phenylenepyridodiimidazole (PIPD), also known as M5, is a high-performance synthetic fiber [1,2]. It has an exceptional fire protection property and the highest compressive strength among all the polymeric fibers, *e.g.*, PBO, Twaron, Kevlar and Nomex fibers [3–6]. The PIPD is synthesized by polycondensation of 2,5-dihydroxy terephthalic acid with 2,3,5,6-tetraaminopyridine (TAP), where the TAP is mainly obtained by hydrogenation of 2,6-diamino-3,5-dinitropyridine (DADNP) [7]. Typically, conventional nitric-sulfuric mixed acids are used for the dinitration of DAP to the target product DADNP [8], whose yield is less than 70% due to side reactions caused by the strong exothermic process or inhibition by the increased water content with the reaction. To address these issues, an extremely concentrated acid system, *i.e.*, 100% nitric acid/20% oleum without other solvents, is required to reduce negative water effects, and the strict safety operation with slowly and intermittently dropwise addition of DAP should be adopted to ensure <5 °C of temperature runaway, achieving the 90.3% yiled of DADNP from DAP dinitration [9,10]. Nevertheless, it remains a challenge in industrial operation which expects a safe and mild system for continuous synthesis of DADNP with high selectivity [11,12].

Notably, only concentrated nitric acid fails to generate DADNP by nitrating DAP, demonstrating the activated role of the mixed acid system in promoting DAP dinitration [13]. Wang *et al.* [14] considered that the existing acid group (HSO_4^- and/or NO_3^-) induces the triazol-3-one nitration with nitronium (NO_2^+) which is in inconformity to typical electrophilic substitution mechanism according to DFT calculation results, and proposed that the relatively dilute acids system is favorable for the formation of inducing species, and thereby yields the considerable target product, *i.e.*, 5-nitro-2,4-dihydro-1,2,4-triazol-3-one (NTO). Moreover, the active role of HSO_4^- on nitration process was confirmed by random combination of wet $Mg(HSO_4)_2$/$NaHSO_4$/ionic liquids [M]HSO_4 with $NaNO_3$/HNO_3 as mild agents for nitration of phenols and aromatics [15–17], but the concrete mechanism also fails to elucidate. Dindi *et al.* [18] proposed the assisted nitration of DAP to obtain 2,6-diamino-3-nitro-5-sulfonic acid pyridine (DANSP) in concentrated nitric acid, which prioritizes to sulphontion of DAP by dissolving it into oleum before nitration [19]. However, it needs to overcome the higher energy barrier of sulphonation, and necessitates further

* Corresponding authors.
E-mail addresses: yzr@ecust.edu.cn (Z. Yang), xzduan@ecust.edu.cn (X. Duan).
# These authors contributed equally to this work.

https://doi.org/10.1016/j.cjche.2022.06.024
1004-9541/

hydrolysis of DANSP in considerable hydrous system to produce mononitriation product, 2,6-diamino-3-nitro-pyridine (DANP). Preferably, the indirect nitration of DAP probably occurs according to the nitration principle of 2-amino-6-methypyridine toward the 2-amino-3-nitro-6-methypyridine, which receives the most approval that the NO_2^+ dissociated from the nitric-sulfuric acid system was suggested as an active intermediate and the amino group was replaced by NO_2^+ to generate $NHNO_2$ group followed by the NO_2 arrangement [20–24].

The aforementioned nitration mechanisms in nitric-sulfuric acid system are generally applied in the nitration system that is used for producing mononitration products. Unclear mechanism of DAP dinitration disorients the high selectivity control of the target product DADNP. To this end, several nitration paths of DAP in the nitric-sulfuric acid system were systematically explored in this study using density functional theory (DFT) calculations, which supports a direct DAP dinitration as optimal path with nitric-hydrogen-sulfate complex (HSO_4^--NO_2^+) coordination. Meanwhile, the evolution of nitration paths affected by the water formation and accompanied thermal effects was suggested, and the reasons for low DAP conversion and DADNP selectivity were clarified. The mechanistic insights into DAP nitration give the comprehensive understanding for the high selectivity control of DADNP, and propose the importance of water content limitation and thermal effects elimination during the reaction, futher confirmed in the batch- and micro-reaction systems.

2. Experimental

2.1. Chemical materials

2,6-Diaminopyridine (DAP, 98%) and dimethyl sulfoxide (DMSO, AR purity) were purchased by Macklin Biochemical Technology Co., Ltd. 65% Nitric acid (65% HNO_3, AR purity), 95% nitric acid (95% HNO_3, AR purity), 98% sulfuric acid (98% H_2SO_4, AR purity), 20% oleum (AR purity), and 50% oleum (AR purity) were purchased by Sinopharm Chemical Reagent Co., Ltd.

2.2. Synthesis of DADNP in the batch reactor and microreactor

DAP/DMSO solution (0.5 mol·L^{-1}, 2–5 ml) was added dropwisely with a feeding rate of 1 ml·min^{-1} into the sulfuric acid/oleum (10–35 ml) in a 100 ml volume three-necked flask with a water jacket at a temperature range of 10–60 °C. After an hour, nitric acid (0.4–1 ml) was added to the reaction solution with a feed rate of 0.5 ml·min^{-1} for nitration. The stirring rate was maintained at 400 r·min^{-1} during the feeding and reaction. Heat transfer fluid flowed around the reactor's external jacket for temperature control. The reaction was terminated after 2 h by adding the proper amount of NaOH to consume the residue acid to ensure pH = 7. For comparison, DADNP was also synthesized in a continuous-flow microreactor to illustrate the side reactions dominated by the thermal effects (Fig. 1) [25,26]. The product analysis was performed using ultraperformance liquid chromatography (UPLC) system (Acquity UPLC; Waters Co., Ltd) using a ZORBAX SB-C18 column. The volume ratio of acetonitrile and water (0.05 mol·L^{-1} NaH_2PO_4, pH = 2.10) in the mobile phase was 40:60. In this study, all yields refer to the UPLC yield, which was calculated by an external standard method. The water content was measured using the Karl Fischer water meter (WKT-C9; VicoMeter Co., Ltd).

2.3. Computational details

All calculations were performed using the Gaussian 09 software package [27]. The geometries of reactant complexes, transition states, and products were optimized using the DFT-M062X method combined with the 6–31 g (d) basis set [28], which has been widely used in a similar system. At the same theoretical levels, vibrational frequencies were calculated on all obtained structures to verify whether they are transition structures or local minima, to provide the zero-point vibrational energy (ZPE), and determine the thermodynamic contributions to enthalpy and free energy. Furthermore, to ensure that the desired reactant and product are connected to the transition structure obtained, an intrinsic reaction coordinate (IRC) [29] analysis was conducted for each transition state. The single-point energies of all stationary points were further calculated at the M06-2X level to obtain more accurate relative energies.

3. Results and Discussion

3.1. Direct nitration of DAP

Synthesis of DADNP *via* the nitration of DAP in the nitric-sulfuric acid system was suggested with NO_2^+ being the active

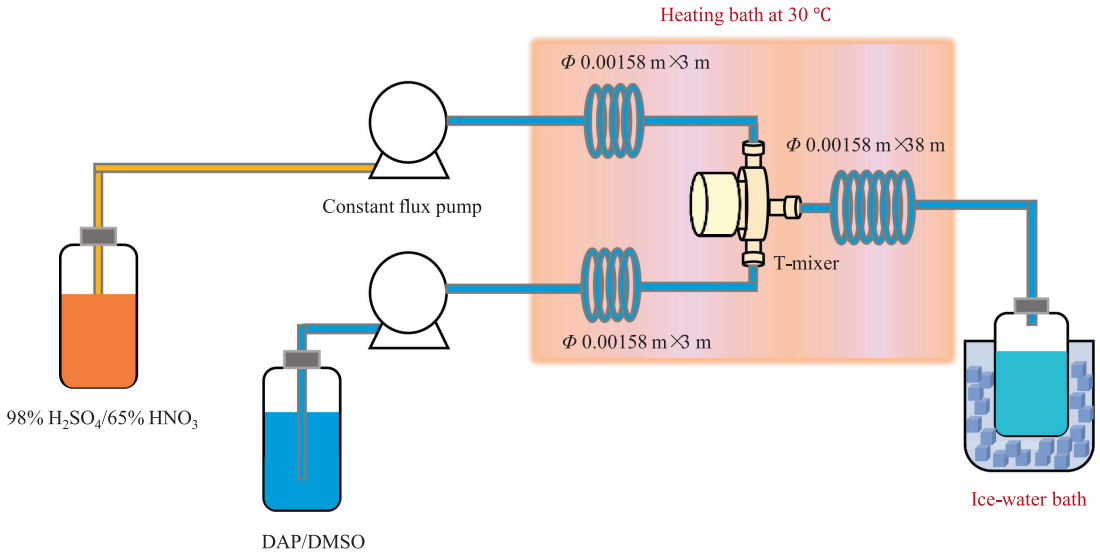

Fig. 1. Continuous-flow microreactor system for DAP dinitration.

phase due to its excellent electrophile compared to the nitric acid system [30]. Typically, the formation of NO_2^+ was considered as the protonation process of $H_2NO_3^+$ in a strong protonic acid system and then dehydrated to form NO_2^+ (Eq. (1)) [31,32]. In the nitric-sulfuric acid system, sulfuric acid acted as an activator to promote the basic ionization of nitric acid, thus increasing the concentration of NO_2^+ and enhancing the nitration capacity. Notably, the formation of water in the mixed acids system changes the complex environment of NO_2^+ from HSO_4^--NO_2^+ to SO_4^{2-}-NO_2^+ (Eqs. (2) and (3)), which inevitably reduces the nitration capacity. Therefore, in such cases, oleum was prioritized for use in the mixed acids system due to the easy absorption of water by SO_3 in oleum and the formation of favorable HSO_4^--NO_2^+ complex (Eq. (4)). Despite the harsh operation in the oleum/concentrated nitric acid system, a considerable amount of water was generated as the reaction proceeds (Fig. 2), which probably changed the active phase of NO_2^+.

$$2HNO_3 \rightleftharpoons NO_3^- + H_2NO_3^+ \rightleftharpoons NO_3^- + NO_2^+ + H_2O \quad (1)$$

$$HNO_3 + H_2SO_4 \rightleftharpoons HSO_4^- - NO_2^+ + H_2O \quad (2)$$

$$HNO_3 + H_2SO_4 \rightleftharpoons SO_4^{2-} - NO_2^+ + H_3O^+ \quad (3)$$

$$SO_3 + HNO_3 \rightleftharpoons HSO_4^- - NO_2^+ \quad (4)$$

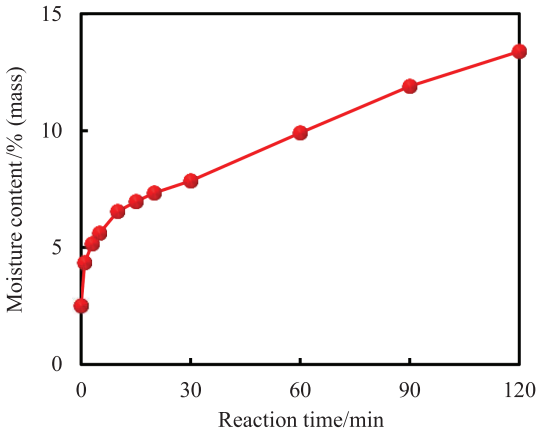

Fig. 2. Water content change in DAP nitration in 50% oleum–65% HNO_3 mixed system.

3.1.1. HNO_3 and NO_2^+ direct nitration

The general mechanism of aromatic nitration using concentrated nitric acid is an electrophilic substitution [8,31–33]. However, the weak pyridine reactivity in electrophilic substitution ascribes to their protonation. Because of their positioning effects, the amino group, as the α-bit (2-, 6-) positioning group in DAP, is preferred to make the β (3- and 5-) substituted product other than the 4-bit nitration due to the inter-NO_2-bit positioning effect. The calculation results (Fig. 3) show that NO_2^+ from HNO_3 directly attacks the C3 atoms (Path A), requiring a high energy barrier (49.08 kcal·mol^{-1}) that would be impossible to achieve at ambient temperature. Furthermore, only the NO_2^+ structure fails to perform the nitration process theoretically (Path B) due to the solitary proton structure in spite of a low energy barrier (19.41 kcal·mol^{-1}). Therefore, DAP nitration in the presence of only concentrated nitric acid is unlikely, which suggests that a proton neutralization complex would stabilize the NO_2^+ structure to promote the nitration process.

3.1.2. HSO_4^--NO_2^+ and SO_4^{2-}-NO_2^+ complexes direct nitration

Fig. 4 shows that the nitration paths C and D involve the formation of HSO_4^--NO_2^+ and SO_4^{2-}-NO_2^+ complexes as the active phase, respectively. According to the water formation trend during DAP nitration (Fig. 2), the active phase of the HSO_4^--NO_2^+ complex gradually changes to SO_4^{2-}-NO_2^+ complex under the influence of water. Path C shows that the HSO_4^--NO_2^+ complex directly attacks the C3 position of DAP with a low energy barrier (10.19 kcal·mol^{-1}), followed by the hydrogen transfer (H13) to HSO_4^- (O19). Typically, H_2SO_4 from the IM2 state continues to combine with nitric acid to form HSO_4^--NO_2^+ complex that further nitrifies the mononitration product (DANP, 2,6-diamino-3-nitro-pyridine) to DADNP with an energy barrier of 17.76 kcal·mol^{-1} (TS3). The nitration path from IM2 to the final state (FS) was similar to that from the initial state to IM2. Notably, the calculations reveal a strongly exothermic process (−54.98 kcal·mol^{-1}) for mononitration, which is sufficient to activate dinitration following the theoretical adiabatic temperature rise (347.26 °C, Table S1 in Supplementary Material), confirming the benefit of the low-temperature operation. In other words, it only needs to overcome 10.19 kcal·mol^{-1} energy barrier of TS1 for dinitration process in the relative adiabatic system, while 17.76 kcal·mol^{-1} energy barrier of TS3 for the final dinitration in the better heat-exchange system. For path D, SO_4^{2-}-NO_2^+ complex also directly attacks the C3 position of DAP as similar to the path C, while the strong electronegativity of SO_4^{2-} intimately attracts the NO_2^+, requiring a small attack distance (0.205 nm between C3 and N16) and thus a high energy barrier of TS1 (59.25 kcal·mol^{-1}).

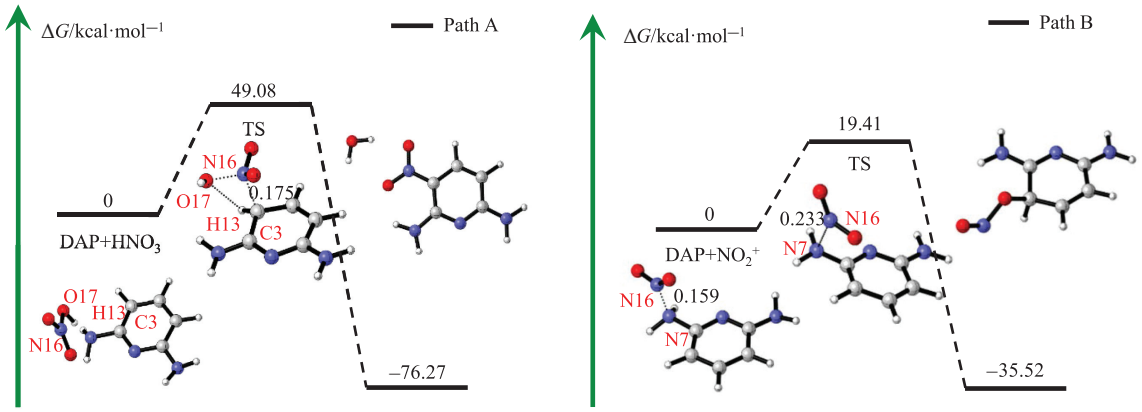

Fig. 3. Schematic energy diagram for the potential energy surface of the (Path A) HNO_3 and (Path B) NO_2^+ direct nitration of DAP in concentrated nitric acid (bond lengths are in nanometer, 1 kcal=4.186 kJ).

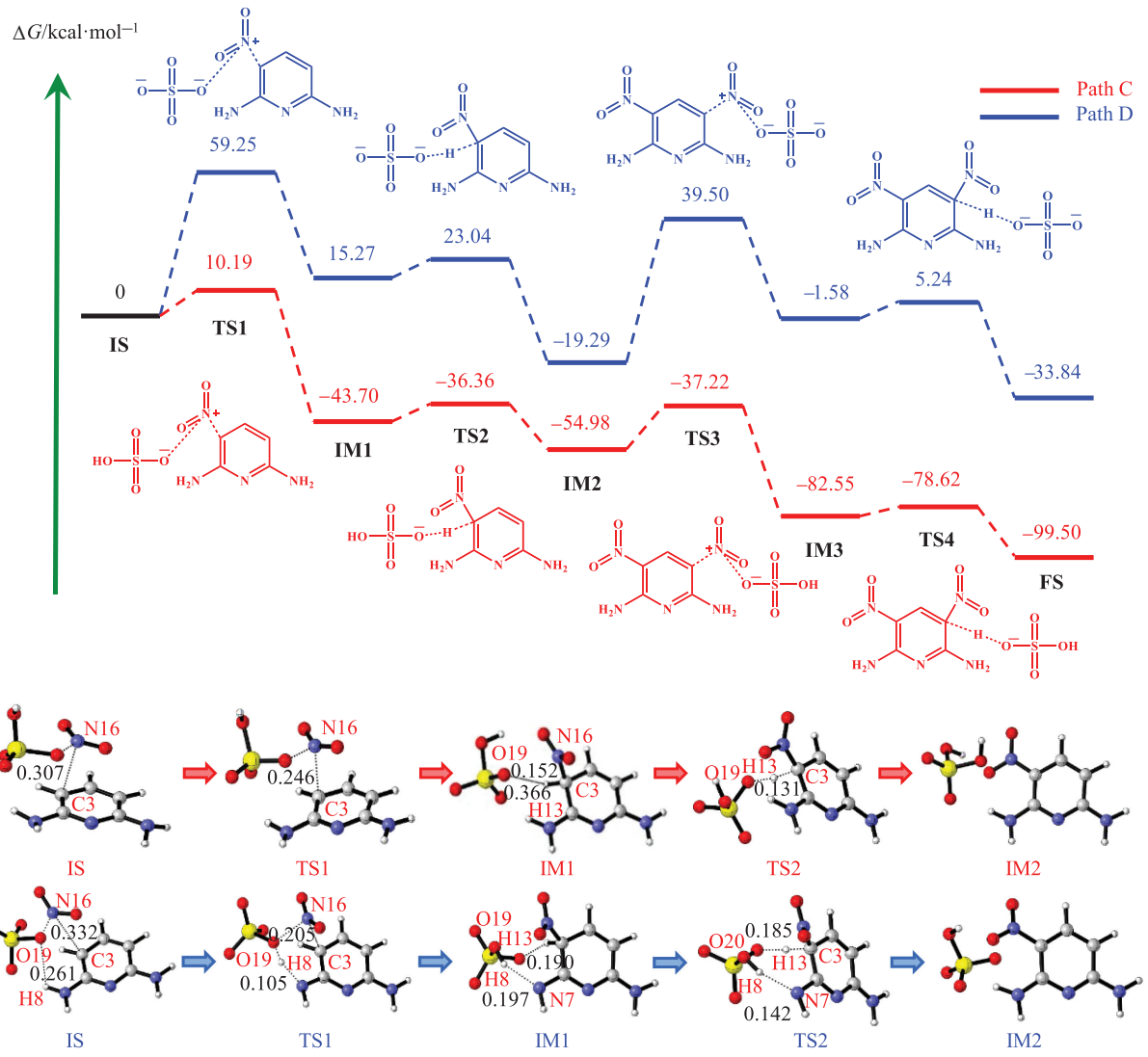

Fig. 4. Schematic energy diagram for the potential energy surface of induced direct nitration of DAP. Path C refers to HSO_4^--NO_2^+ complex direct nitration. Path D refers to SO_4^{2-}-NO_2^+ complex direct nitration (bond lengths are in nanometer, 1 kcal=4.186 kJ).

Noticeably, the easy hydrogen transfer (H8) in amino group of DAP caused by the strong electronegativity of SO_4^{2-} contributes to the extreme energy barrier of TS1, which significantly exceeds the energy barrier of HNO_3 direct nitration (49.08 kcal·mol^{-1}, Fig. 3 Path A). Following the mononitration, the reversible hydrogen transfer (H8) occurs with ease, overcoming the 7.8 kcal·mol^{-1} energy barrier from IM1 to TS2. The dinitration path from IM2 to FS follows the same trend as the mononitration path, which still overcomes the energy barrier of 58.79 kcal·mol^{-1}. The above results indicate the significance of HSO_4^- in promoting DAP nitration to form DADNP.

3.2. Indirect nitration of DAP

The nitration of 2-aminopyridine (AP) is reported to be divided into two parts: the formation of $NHNO_2$ intermediates and the nitro rearrangement [9]. Therefore, we further considered this indirect nitration mechanism of DAP induced by HSO_4^-. In the presence of HSO_4^-, the hydrogen transfer on the amino group (H8 on N7) easily occurred and was attracted by HSO_4^-, making the N7 position vulnerable to $NHNO_2$ intermediate formation with the attachment of NO_2^+ to the target N7 atom (Fig. 5). Concurrently, the protonation of HSO_4^- as the medium easily releases the hydrogen proton for transfering to the pyridine-nitrogen. The formation of one $NHNO_2$ structure only overcomes an energy barrier of 11.37 kcal·mol^{-1}, making it difficult to distinguish the best path compared with path C (direct nitration). Nevertheless, the next nitration step has two paths: one is the continuous formation of two $NHNO_2$ structures (Path E) and the other is nitro rearrangement once one $NHNO_2$ intermediate is formed (Path F). The significant difference in the energy barriers of TS2 for both paths (8.14 kcal·mol^{-1} and 33.14 kcal·mol^{-1}) confirms that two $NHNO_2$ structures can be formed rather than nitro rearrangement. However, it has a high energy barrier for further nitro rearrangement (70.13 kcal·mol^{-1}, TS3 in Path E), inhibiting DADNP formation. Alternatively, 2,6-dinitraminopyridine (pyridine-2$NHNO_2$) is the FS of the indirect DAP nitration in terms of calculation results. Notably, hydrogen transfer in DAP indirect nitration frequently necessitates the use of pyridine-nitrogen as a releasing medium to the proton acceptor (SO_4^{2-}), which only overcomes a 7.97 kcal·mol^{-1} energy barrier (IM2 to IM3 in Path F). Comparably, without the proton-releasing medium of pyridine-nitrogen, the formation of the second $NHNO_2$ structure and subsequent nitro rearrangement must overcome energy barriers of 16.49 kcal·mol^{-1} and 81.43 kcal·mol^{-1}, respec-

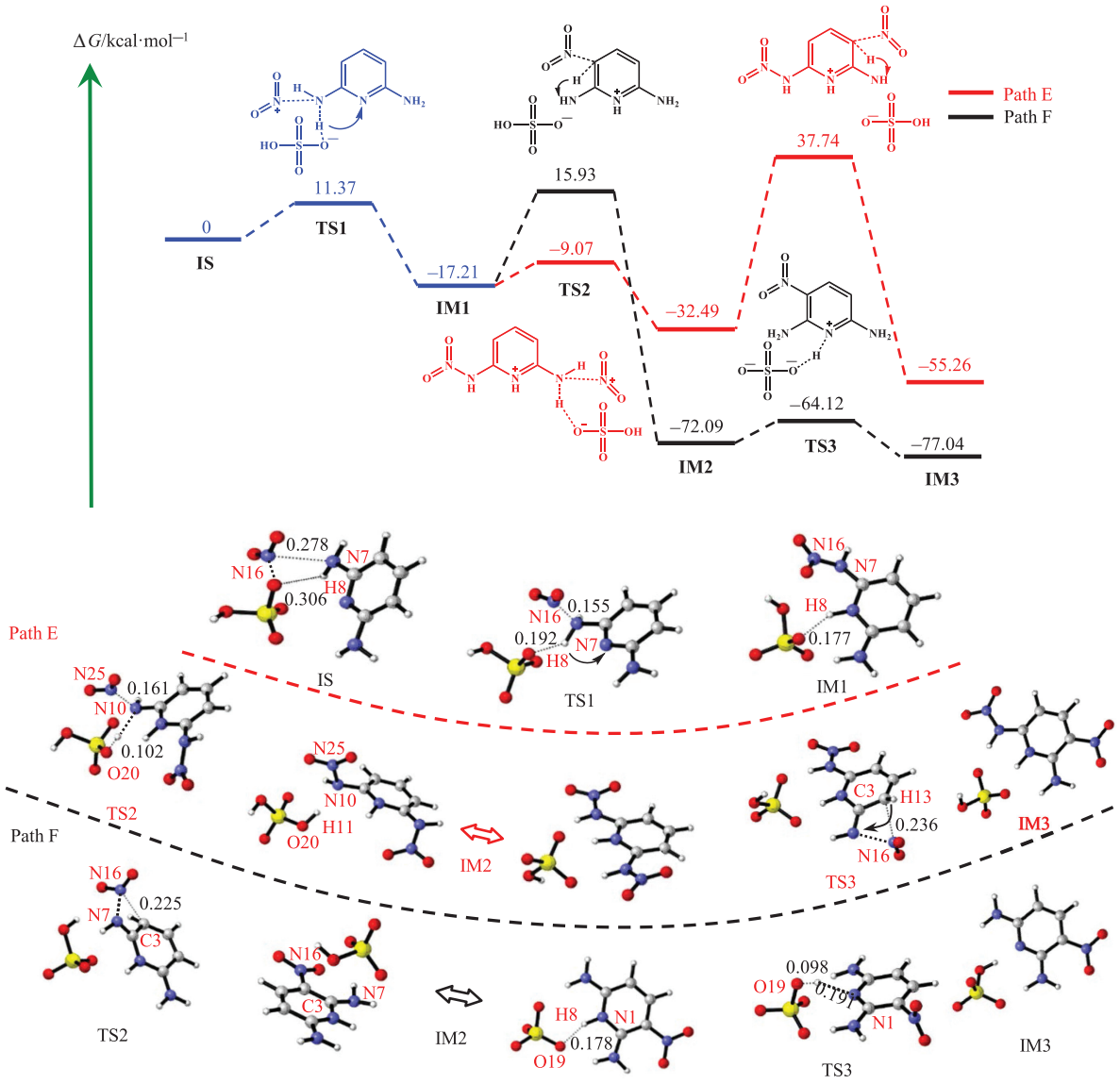

Fig. 5. Schematic energy diagram for potential energy surface of HSO_4^--NO_2^+ indirect nitration of DAP. Path E refers to nitro rearrangement after two $NHNO_2$ intermediate formations, Path F refers to nitro rearrangement with one $NHNO_2$ intermediate formation (bond lengths are in nanometer, 1 kcal=4.186 kJ).

tively (Path G in Fig. S1). From the energetic perspective, DAP's indirect nitration path easily converts DAP to pyridine-$NHNO_2$ but fails to obtain the target product, DADNP.

3.3. Assisted nitration of DAP

The priority of DAP sulfonation by oleum to create DAP-SO_3H intermediate, followed by subsequent nitration, has been described in the oleum/concentrated nitric acid system [17]. Typically, SO_3 in the oleum is the active phase to sulfonate the aromatics. Consequently, DAP sulfonation by SO_3 should overcome the energy barrier of 34.96 kcal·mol^{-1} (TS1 in Fig. 6). The subsequent nitration presents the energy barriers of 51.35, 40.36, and 15.08 kcal·mol^{-1} if the nitrating active phases are HNO_3, SO_4^{2-}-NO_2^+, and HSO_4^--NO_2^+ complexes, respectively. This assisted nitration path indicates the accessibility of SO_4^{2-}-NO_2^+ complexes that reduces the energy barrier compared with the direct nitration of SO_4^{2-}-NO_2^+ complexes (59.25 kcal·mol^{-1} in Fig. 4 Path D). However, the mononitration product from the assisted nitration path is difficult to continue nitration to obtain the target product, since the hydrolysis removal of the sulfonic acid group requires a substantial amount of water. Therefore, this assisted nitration path results in the stability of the mononitration product, DANP. Because the HSO_4^--NO_2^+ complex is more likely to transform into the SO_4^{2-}-NO_2^+ complex as water content increases during the reaction, direct nitration fails. Thus, the assisted nitration of DAP by SO_4^{2-}-NO_2^+ complexes may occur if there is sufficient heat accumulation in the mixed acid system to activate DAP sulfonation.

Various nitration systems with different water contents were used to confirm the aforementioned DAP nitration mechanism. Table 1 shows that concentrated nitric acid (65%) does not activate the nitration process at ambient temperature (entry 1), whereas 95% nitric acid only contributes to a low DAP conversion (4.7%, entry 2), corresponding to the high energy barrier from calculation results (Path A in Fig. 3). Both entries 3 and 4 achieve similar DAP conversion and DADNP selectivity with a sequence change of 98% sulfuric acid and 65% nitric acid in the mixed system, indicating the same nitration mechanisms free from the sulfonic group's control before the reaction. However, the low DAP conversion and DADNP selectivity (about 80%) are attributed to the sharp increase

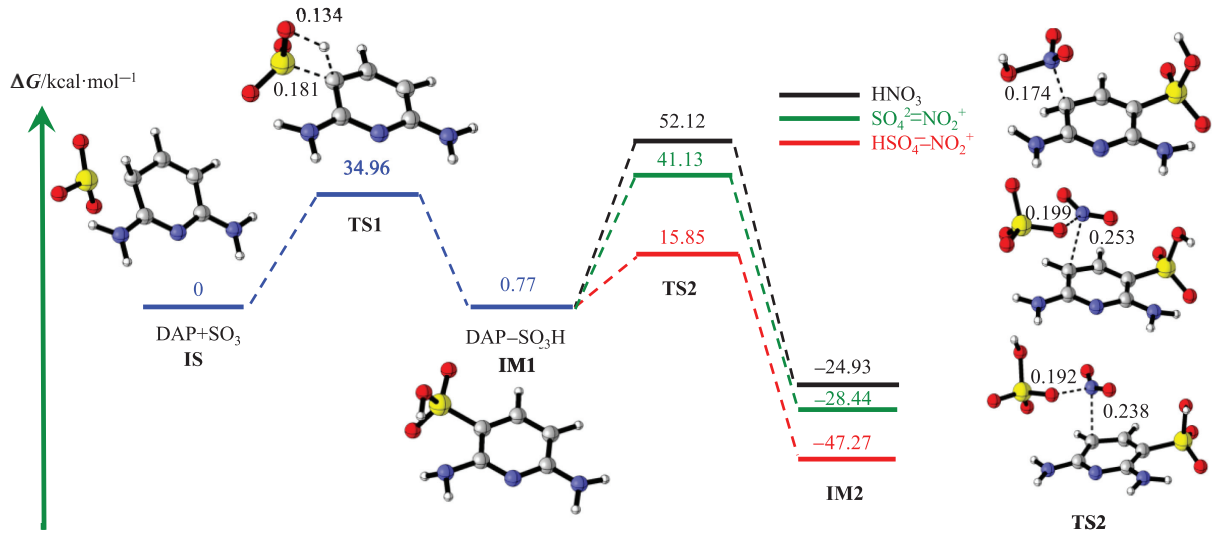

Fig. 6. Schematic energy diagram for the potential energy surface of assisted nitration of DAP-SO_3H in HNO_3, SO_4^{2-}-NO_2^+, and HSO_4^--NO_2^+ complex system (bond lengths are in nanometer, 1 kcal=4.186 kJ).

Table 1
Effects of different nitration systems on the nitration of DAP

Entry	Nitration system	DAP conver./%	DADNP select. ①/%	H_2O content before reaction② /%(mass)	H_2O content after reaction /%(mass)
1	65% HNO_3	0	0	7.59	8.01
2	95% HNO_3	4.80	15.21	6.03	7.21
3	65% HNO_3/98% $H_2SO_4$③	80.75	80.17	7.42	20.97
4	98% H_2SO_4/65% HNO_3	82.68	79.54	3.01	21.78
5	98% H_2SO_4/65% HNO_3/H_2O ④	59.54	57.63	7.54	26.03
6	20% Oleum/65% HNO_3	84.15	84.92	2.64	13.54
7	50% Oleum/65% HNO_3	84.07	85.53	2.51	13.39
8	50% Oleum/95% HNO_3	89.15	90.87	2.46	12.89
9	$NaHSO_4$/65% HNO_3 ⑤	0	0	-	-

Note: Reaction temperature = 30 °C, reaction time = 2 h, molar ratio of H_2SO_4 (oleum) and HNO_3 to DAP = 250:2.2:1. The concentration of DAP in the DMSO solution was 0.5 mol·L^{-1}.
① The total selectivity of DANDP and DANP is 100%.
② The H_2O content before the reaction was measured after mixing DAP and oleum (H_2SO_4).
③ In entry 3, HNO_3 was added before H_2SO_4. The H_2O content before the reaction was measured after mixing DAP and HNO_3.
④ The additional H_2O content in entry 5 was 4.5% (mass).
⑤ $NaHSO_4$/CH_2Cl_2 solution, the equivalent molar amount of $NaHSO_4$ to 98% H_2SO_4 in entry 4.

of water content in the system from 3.01% (mass) to 21.78% (mass). Comparably, DAP conversion and DADNP selectivity rapidly reduce to 59.54% and 57.63%, respectively, if 4.5% (mass) water is added to the mixed acid system before the reaction (entry 5). Accordingly, replacing 98% H_2SO_4 with oleum could further improve DAP conversion and DADNP selectivity due to the small water content in the acid system (entries 6–8). However, the water content limit reduces to 2.46% in the high concentration of oleum and nitric acid systems (50% oleum/95% HNO_3), which achieves 89.15% DAP conversion and 90.87% DADNP selectivity. No further improvement in DAP reaction performance was attributed to the water tolerance in the system, which inevitably generates at least 10% (mass) water content and thus changes the nitration mechanism by tuning the nitrating active phase and triggering various side reactions. In view of the strict requirement for water tolerance in acids system, the reported mild sulfonation reagent, $NaHSO_4$ [15–17], fails to induce the DAP nitration compared with same acids system (entry 9 *vs.* entry 4) due to the non-free HSO_4^- in water-limited system that is unable to generate the favorable HSO_4^--NO_2^+ complex.

3.4. Experiential verification of DAP nitration

Given the above-proposed nitration mechanisms for DAP, the optimal synthesis parameters were further confirmed by experiential verification, including reaction temperature, molar ratios of oleum and nitric acid to DAP, and reaction time. The unexpected trends in the reaction performance reveal the tunable nitration mechanism as the reaction proceeds. Fig. 7(a) shows that DAP conversion increased from 70.34% to a maximum of 90.44% as the reaction temperature increased from 10 °C to 40 °C, followed by a decrease as the temperature further increased. Meanwhile, the DADNP selectivity was also reduced at temperatures between 40 °C and 60 °C. This indicates that the high reaction temperature easily activates the assisted and indirect nitrations as heat accumulation and water formation increase. Assisted nitration produces the mononitration product (DANP) with lower DADNP selectivity, whereas indirect nitration results in low DAP conversion due to the difficult rearrangement of pyridine-$NHNO_2$ to DADNP at high reaction temperatures. Fig. S2 demonstrates the reversible change of pyridine-$NHNO_2$ and DAP in terms of the energy barrier (40.14 kcal·mol^{-1}) if the assisted nitration occurs in the system (41.13 kcal·mol^{-1}). This unstable pyridine-$NHNO_2$ was difficult to detect from the experimental attempts even at −5 °C careful operation. However, DANP-SO_3H intermediate was detected by LC-MS (Fig. S3) without neutralization treatment, and it easily transfers into DANP after solution neutralization, demonstrating the role of assisted nitration on the production of DANP. Increased oleum consumption in the system can lower

water tolerance, which improves the DAP reaction performance to some extent. However, Fig. 7(b) shows that the optimal DAP reaction performance was achieved at oleum to DAP mole ratio of 250:1. Similarly, the DAP conversion and DADNP selectivity were both reduced at a higher ratio (>250:1) because the abundant SO_3 in the oleum activates the assisted nitration when the water content achieves a low equilibrium limit by SO_3 adsorption. Comparably, the optimal performance is achieved at an HNO_3 to DAP mole ratio of 2.2 (Fig. 7(c)), and it also maintains a stable performance at higher ratios (>2.2:1), showing that the nitration mechanism does not change when the usage of HNO_3 is increased. Furthermore, it confirms that the nitration duration should be more than 2 h to accomplish nitration given the complicated nitration paths (Fig. 7(d)).

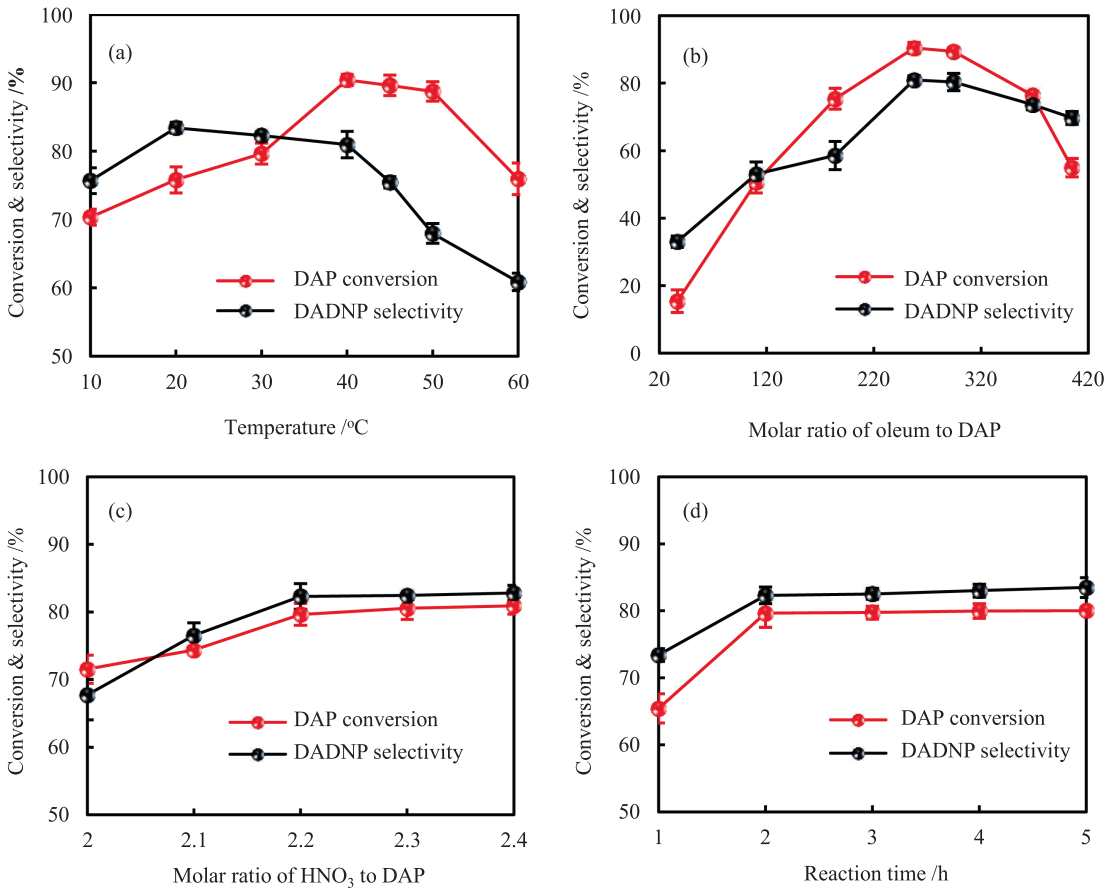

Fig. 7. Effects of (a) temperature, (b) molar ratio of oleum to DAP, (c) molar ratio of HNO_3 to DAP, and (d) reaction time on the DAP nitration. Conditions: (a) molar ratios of oleum and HNO_3 to DAP = 250:2.2:1, reaction time = 2 h; (b) temperature = 30 °C, molar ratio of HNO_3 to DAP = 2.2:1, reaction time = 2 h; (c) temperature = 30 °C, and molar ratio of oleum to DAP = 250:1; (d) temperature = 30 °C, molar ratios of oleum and HNO_3 to DAP = 250:2.2:1.

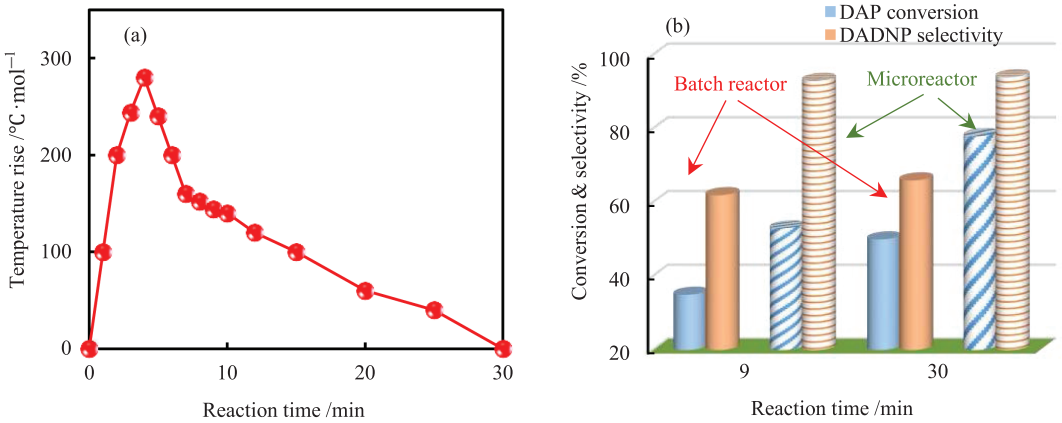

Fig. 8. (a) Temperature rise as DAP nitration progresses, (b) comparison of DAP nitration performance conducted in the batch and microreactors. Conditions in the batch reactor are as follows: molar ratios of 98% H_2SO_4 and 65% HNO_3 to DAP = 250:20:1, DAP concentration in DMSO solution is 0.5 mol·L^{-1}, temperature = 30 °C; Conditions in the microreactor are as follows: flow rates of DAP/DMSO solution (first stream) and 98% H_2SO_4/65% HNO_3 solution (second stream) are 2 and 0.25 ml·min^{-1}, respectively, molar ratios of 98% H_2SO_4 and 65% HNO_3 to DAP = 250:20:1, DAP concentration in DMSO solution is 0.5 mol·L^{-1}, temperature = 30 °C, the microchannel of the microreactor system is a 1/16-inch pipe.

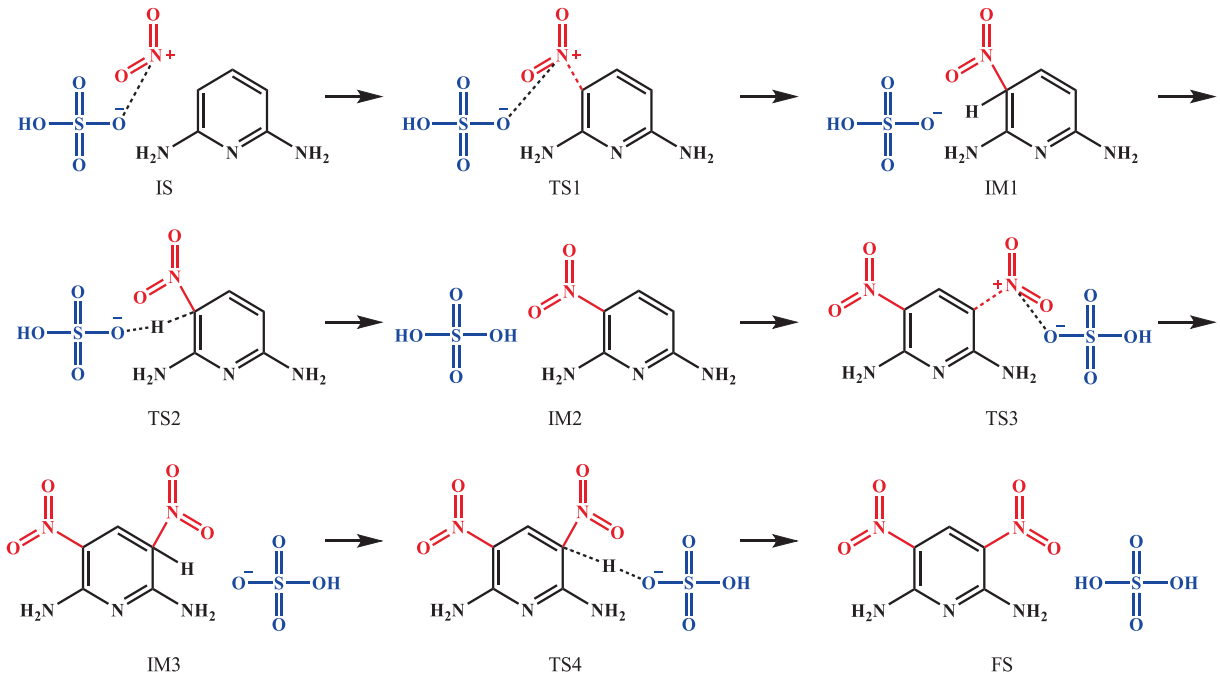

Fig. 9. Synthesis path of DADNP from direct nitration of DAP with HSO−4-NO+2complex coordination.

The temperature increase was measured due to the negative effects of temperature out-of-control on the DAP nitration in a batch reactor. Fig. 8(a) shows that the maximum temperature rise is 282 °C per mole of DAP (the theoretical adiabatic temperature rise is 347.26 °C, Table S1), implying that the side reaction and assisted nitration are easily caused by high thermal effects. The DAP nitration performance was evaluated in a continuous-flow microreactor for comparison, where the thermal effects were minimized due to the excellent mass and heat transfer capacity (the calculated temperature rise is 0.47 °C, Table S2). Fig. 8(b) shows that the DAP conversion and DADNP selectivity achieved 78% and 94%, respectively, in 30 min in the microreactor, whereas they achieved 50% and 63%, respectively, in the batch reactor under the same conditions, demonstrating the thermal effects on DADNP selectivity.

Overall, DAP nitration allows for various paths if the system is out of temperature control, converting direct nitration to indirect nitration based on their approximate energy barriers (10.19 and 11.37 kcal·mol^{-1}), thus limiting the DAP conversion. Furthermore, the assisted nitration was easily initiated with the water formation, generating mononitration byproducts and decreasing DADNP selectivity. Therefore, designing a reactor with precise temperature control and good mass/heat transfer effects would significantly improve the DAP reaction performance, as it follows the direct nitration mechanism (Fig. 9), in which the favorable HSO_4^--NO_2^+ complex is maintained as the active phase throughout the reaction.

4. Conclusions

The mechanistic insights into the DAP nitration is beneficial for the high selectivity control of DADNP. Various DAP nitration paths in the nitric-sulfuric acid system were identified using DFT with the M06-2X functional. The results show that the favorable HSO_4^--NO_2^+ complex initiates the direct nitration *via* the optimal path with low energy barrier (*i.e.*, 10.19 kcal·mol^{-1}). The formed water during the reaction leads to the formation of less active SO_4^--NO_2^+ complex and the assisted nitration path through which the mononitration byproducts were generated after DAP sulfonation (DAP-SO_3H intermediate), thus decreasing DADNP selectivity. Meanwhile, the accompanied thermal effects easily initiate indirect nitration *via* amino-nitration (pyridine-$NHNO_2$ intermediate) which is difficult to be rearranged to DADNP, inhibiting the reaction and thus resulting in low DAP conversion. This mechanistic understanding of the DAP nitration elucidates the importance of thermal effects elimination and water content control for high DAP conversion and DADNP selectivity.

Declaration of Competing Interest

The authors declare that they have no known competing financial interests or personal relationships that could have appeared to influence the work reported in this paper.

Acknowledgements

This work was financially supported by the National Natural Science Foundation of China, China (21922803, 22122807, and 22008072), the Innovation Program of Shanghai Municipal Education Commission, China, the Program of Shanghai Academic/Technology Research Leader, China (21XD1421000), the China Postdoctoral Science Foundation, China (2020M671025 and 2019TQ0093).

Supplementary Material

Supplementary data to this article can be found online at https://doi.org/10.1016/j.cjche.2022.06.024.

References

[1] Z.F. Li, F. Lu, S.S. Lu, H. Liu, B.Y. An, Y.H. Wang, Y.D. Huang, Z. Hu, Fabrication of uvioresistant poly(*p*-phenylene benzobisoxazole) fibers based on hydrogen bond, *J. Appl. Polym.* 137 (9) (2020) 48432.
[2] N. Taloub, L. Liu, N. Rahoui, M. Hegazy, Y.D. Huang, Grafting multi-walled carbon nanotubes (MWCNTs) into PIPD fiber for enhancing mechanical and interfacial performance, *Polym. Test.* 75 (2019) 344–349.
[3] S.R. Fu, B.W. Yu, L.Y. Duan, H.W. Bai, F. Chen, K. Wang, H. Deng, Q. Zhang, Q. Fu, Combined effect of interfacial strength and fiber orientation on mechanical

performance of short Kevlar fiber reinforced olefin block copolymer, *Compos. Sci. Technol.* 108 (2015) 23–31.
[4] T. Zhang, J.H. Jin, S.L. Yang, G. Li, J.M. Jiang, Preparation and properties of novel PIPD fibers, *Chin. Sci. Bull.* 55 (2010) 4203–4207.
[5] N. Taloub, L. Liu, Y.Z. Du, N. Rahoui, Y.D. Huang, Surface modification of PIPD fiber using nitric acid treatment, *Surf. Coat. Technol.* 334 (2018) 312–318.
[6] Y. Wang, Y.J. Song, L. Zhao, N. Rahoui, B. Jiang, Y.D. Huang, An investigation of the high performance of a novel type of benzobisoxazole fiber based on 3,3-diaminobenzidine, *Polymers* 8 (12) (2016) 420–431.
[7] R.L. Williams, S.A. Cohen, The chemistry of aryltetraamines. II. The synthesis of 2,3,5,6-tetraaminopyridine, *J. Heterocycl. Chem.* 8 (5) (1971) 841–843.
[8] B. Galabov, D. Nalbantova, P.V.R. Schleyer, H.F. Schaefer, Electrophilic aromatic substitution: New insights into an old class of reactions, *Acc. Chem. Res.* 49 (6) (2016) 1191–1199.
[9] H. Ritter, H.H. Licht, Synthesis and reactions of dinitrated amino and diaminopyridines, *J. Heterocycl. Chem.* 32 (2) (1995) 585–590.
[10] D.J. Sikkema, Nitration of pyridine-2, 6-diamines, US Pat., 05945537 (1999).
[11] X. Peng, H. Suzuki, Regioselective double kyodai nitration of toluene and chlorobenzene over zeolites. High preference for the 2,4-dinitro isomer at the second nitration stage, *Org. Lett.* 3 (22) (2001) 3431–3434.
[12] D.J. Martin, B.Q. Mercado, J.M. Mayer, Synthesis and prior misidentification of 4-tert-butyl-2,6-dinitrobenzaldehyde, *J. Org. Chem.* 84 (18) (2019) 12172–12176.
[13] O.C. Van Der Jagt, A. Beukers, The potential of a new rigid-rod polymer fibre ('M5') in advanced composite structures, *Polymer* 40 (4) (1999) 1035–1044.
[14] K. Wang, J.G. Chen, B. Wang, F. Liu, Z.T. Liu, Z.W. Liu, W. Wang, J. Jiang, Z. Hao, J. Lu, Density functional theory study on the reaction of triazol-3-one with nitronium: Direct nitration versus acidic group-induced nitration, *RSC Adv.* 5 (32) (2015) 25183–25191.
[15] M.A. Zolfigol, E. Ghaemi, E. Madrakian, Nitration of phenols under mild and heterogeneous conditions, *Molecules* 6 (7) (2001) 614–620.
[16] X.L. Zhou, Z.L. Liu, J. Cheng, X.F. Zhao, Study on the nitration reaction of 2,6-diacetamidopyrazine-1-oxide, *Explos. Mater.* 43 (4) (2014) 16–21.
[17] G.B. Cheng, X.L. Duan, X.F. Qi, C.X. Lu, Nitration of aromatic compounds with NO_2/air catalyzed by sulfonic acid-functionalized ionic liquids, *Catal. Commun.* 10 (2) (2008) 201–204.
[18] H. Dindi, A.J. Schultz, Synthesis of diaminodinitropyridine, *Europe Pat.* 2217570 (2012).
[19] G. Koleva, B. Galabov, J. Kong, H.F. Schaefer, P.V.R. Schleyer, Electrophilic aromatic sulfonation with SO_3: Concerted or classic SEAr mechanism?, *J Am. Chem. Soc.* 133 (47) (2011) 19094–19101.
[20] M. Afshari, D. Sikkema, K. Lee, M. Bogle, High performance fibers based on rigid and flexible polymers, *Polym. Rev.* 48 (2) (2008) 230–274.
[21] T.Z. Chen, Y.L. Ge, Y.C. Liu, H. He, N-nitration of secondary aliphatic amines in the particle phase, *Chemosphere* 293 (2022) 133639.
[22] M. Tanaka, E. Muro, H. Ando, Q. Xu, M. Fujiwara, Y. Souma, Y. Yamaguchi, NO_2^+ nitration mechanism of aromatic compounds: Electrophilic *vs* charge-transfer process, *J. Org. Chem.* 65 (10) (2000) 2972–2978.
[23] B. Rodenko, M. Koch, A.M. Van Der Burg, M.J. Wanner, G.-J. Koomen, The mechanism of selective purine C-nitration revealed: NMR studies demonstrate formation and radical rearrangement of an N7-nitramine intermediate, *J. Am. Chem. Soc.* 127 (16) (2005) 5957–5963.
[24] G. Koleva, B. Galabov, B. Hadjieva, H.F. Schaefer Iii, P.V.R. Schleyer, An experimentally established key intermediate in benzene nitration with mixed acid, *Angew. Chem. Int. Ed.* 54 (47) (2015) 14123–14127.
[25] J.N. Shen, Y.C. Zhao, G.W. Chen, Q. Yuan, Investigation of nitration processes of iso-octanol with mixed acid in a microreactor, *Chin. J. Chem. Eng.* 17 (3) (2009) 412–418.
[26] Z.F. Yan, J.X. Tian, C.C. Du, J. Deng, G.S. Luo, Reaction kinetics determination based on microfluidic technology, *Chin. J. Chem. Eng.* 41 (2022) 49–72.
[27] M.J. Frisch, G.W. Trucks, H.B. Schlegel, G.E. Scuseria, M.A. Robb, J.R. Cheeseman, G. Scalmani, V. Barone, G.A. Petersson, H. Nakatsuji, X. Li, M. Caricato, A.V. Marenich, J. Bloino, B.G. Janesko, R. Gomperts, B. Mennucci, H.P. Hratchian, J.V. Ortiz, A.F. Izmaylov, J.L. Sonnenberg, Williams, F. Ding, F. Lipparini, F. Egidi, J. Goings, B. Peng, A. Petrone, T. Henderson, D. Ranasinghe, V.G. Zakrzewski, J. Gao, N. Rega, G. Zheng, W. Liang, M. Hada, M. Ehara, K. Toyota, R. Fukuda, J. Hasegawa, M. Ishida, T. Nakajima, Y. Honda, O. Kitao, H. Nakai, T. Vreven, K. Throssell, J.A. Montgomery Jr., J.E. Peralta, F. Ogliaro, M.J. Bearpark, J.J. Heyd, E. N. Brothers, K.N. Kudin, V.N. Staroverov, T.A. Keith, R. Kobayashi, J. Normand, K. Raghavachari, A.P. Rendell, J.C. Burant, S.S. Iyengar, J. Tomasi, M. Cossi, J.M. Millam, M. Klene, C. Adamo, R. Cammi, J.W. Ochterski, R.L. Martin; K. Morokuma, O. Farkas, J.B. Foresman, D.J. Fox, Gaussian 09, Revision D.01, Wallingford, CT, 2010.
[28] A.M. Elhorri, M. Zouaoui-Rabah, NLO response of derivatives of benzene, stilbene and diphenylacetylene: MP2 and DFT calculations, *Chin. J. Chem. Eng.* 25 (6) (2017) 800–808.
[29] C. Gonzalez, H. Schlegel, An improved algorithm for reaction-path following, *J. Chem. Phy.* 90 (4) (1989) 2154–2161.
[30] E.L. Blackall, E.D. Hughes, N-nitration and C-nitration by the nitronium ion, *Nature* 170 (4336) (1952) 972–973.
[31] F. Cacace, M. Attina, G. De Petris, M. Speranza, Protonated nitric acid. Structure and relative stability of isomeric $H_2NO_3^+$ ions in the gas phase, *J. Am. Chem. Soc.* 112 (3) (1990) 1014–1018.
[32] J.F.D. Queiroz, J.W.D.M. Carneiro, A.A. Sabino, R. Sparrapan, M.N. Eberlin, P.M. Esteves, Electrophilic aromatic nitration: Understanding its mechanism and substituent effects, *J. Org. Chem.* 71 (16) (2006) 6192–6203.
[33] Y.J. Peng, Y.X. Jiang, X. Peng, J.Y. Liu, W.P. Lai, Reaction mechanism of 3,4-dinitrofuroxan formation from glyoxime: dehydrogenation and cyclization of oxime, *ChemPhysChem* 17 (4) (2016) 541–547.